Biochemical and Biophysical Research Communications 809 (2026) 153492

Contents lists available at ScienceDirect

Biochemical and Biophysical Research Communications

journal homepage: www.elsevier.com/locate/ybbrc

Targeting Warburg effect: involvement of lactate transporter MCT1 and its chaperone in cancer cell killing by 18β-glycyrrhetinic acid

Bingxin Xia [a], Chen Zhu [a,b], Yi Rao [a,b,*]

[a] Academy for Advanced Interdisciplinary Studies, Department of Chemical Biology, College of Chemistry and Chemical Engineering, School of Pharmaceutical Sciences, Peking-Tsinghua Center for Life Sciences, School of Life Sciences, PKU-IDG/McGovern Institute for Brain Research, Peking University, Beijing, 100871, China
[b] Chinese Institutes for Medical Research, Capital Medical University, and Chinese Institute for Brain Research, Zhongguanchun Life Sciences Park, Beijing, China

ARTICLE INFO

JEL classification:
Biological Sciences
Cell Biology
Pharmacology

Keywords:
Warburg effect
cancer
Transporters
Chinese herb medicine

ABSTRACT

One of the most commonly used Chinese medicinal herbs is licorice, whose major component is glycyrrizic acid, with a derived product 18β-glycyrrhetinic acid (18β-GA) possessing antitumor activity. Here we performed a genome-wide CRISPR screen to identify genes required for 18β-GA sensitivity. We discovered involvement of MCT1, a lactate transporter, and its membrane chaperone basigin (BSG) in 18β-GA killing of cancer cells. MCT1 was necessary and sufficient for 18β-GA uptake by cancer cells. BSG was required for MCT1 localization on the membrane, and hence 18β-GA uptake into and death of, cancer cells. While it is known that Warburg effects in cancers increased lactate production, followed by selection of higher MCT1 expression which enhanced cancer cell survival by exporting lactate, our findings reveal a new opportunity for killing cancer cells by increased 18β-GA sensitivities of cancer cells with higher MCT1 expression due to the Warburg effect. Thus, our results have revealed a biomarker for 18β-GA sensitivity and suggested the possibility of using Warburg effect to allow drug entry into tumor cells, and will stimulate further molecular mechanistic studies and improvements of traditional Chinese herb medicines.

1. Introduction

Traditional Chinese medicine has helped China for thousands of years before the introduction of modern medicine. Among the most often used Chinese herb medicines is licorice (*Glycyrrhiza glabra*), which has a long history [1,2]. The major chemical extracted from its root is glycyrrizic acid, which is hydrolyzed by intestinal bacteria to 18β-glycyrrhetinic acid (18β-GA) [3,4].

Cancer continues to pose a significant challenge to global health, with conventional treatments often constrained by drug resistance and adverse effects. A hallmark of cancer cell metabolism was discovered by Otto Warburg a hundred years ago [5–7], and soon confirmed by Carl and Getty Coris [8–12]. It was initially thought that glycolysis was increased whereas oxidative phosphorylation, but later consensus is that only glycolysis is increased, even under aerobic conditions in cancer cells ("aerobic glycolysis), with increased production of lactate [5–7,10,11].

The discovery of novel therapeutic agents and molecular targets is crucial for advancing cancer treatment. Several noteworthy anticancer drugs have been discovered from plants, such as paclitaxel and vinca alkaloids, which have ultimately become first-line treatment options for common cancers like ovarian cancer [13]. 18β-GA has been found to have anticancer effects [14,15], exhibiting broad-spectrum activities against multiple cancer cells [16–19]. 18β-GA can inhibit major pathways essential for cancer growth and metastasis, such as PI3K/Akt, MAPK/ERK1/2, and Akt/mTORC1/STAT3 [14,17,20,21]. While there is much research on the anticancer mechanisms of 18β-GA, little is known about molecular basis on the cell membrane which allows 18β-GA entry into the cell [22–24].

CRISPR-Cas9 provides a powerful technology to modify genes [25] and a derived technique is to apply CRISPR-Cas9 for functional screening of genes [26–30]. It can be used to find the mechanisms underlying drug sensitivity and resistance [29,31,32].

In this study, we applied CRISPR-Cas9 based screening to systematically search for genes required for 18β-GA responsiveness. We found monocarboxylate transporter 1 (MCT1, also known as SLC16A1), and its

* Corresponding author. Academy for Advanced Interdisciplinary Studies, Department of Chemical Biology, College of Chemistry and Chemical Engineering, School of Pharmaceutical Sciences, Peking-Tsinghua Center for Life Sciences, School of Life Sciences, PKU-IDG/McGovern Institute for Brain Research, Peking University, Beijing, 100871, China.
E-mail address: yrao@pku.edu.cn (Y. Rao).

https://doi.org/10.1016/j.bbrc.2026.153492
Received 3 December 2025; Received in revised form 16 February 2026; Accepted 17 February 2026
Available online 17 February 2026

membrane chaperone basigin (BSG) to be required for 18β-GA sensitivity.

Solute carriers (SLC) contribute to both cytoplasmic and vesicular transporters. Family 16 (SLC16) has 14 members in humans and they are secondary active transporters relying on electrochemical Na^+ or H^+ gradients [33–36]. MCT1, a member of SLC16, is a proton-coupled transporter for monocarboxylic acids such as lactate and pyruvate [37–41]. BSG is the chaperone for MCTs and is crucial for the membrane localization of MCT1, MCT3, and MCT4 [42–47]. Overexpression of MCT1 has been found in cancers [36,48–56]. MCT1 allows transport of lactic acid out of cancers undergoing aerobic glycolysis, which is critical for cancer cell metabolism. A previous strategy to target the Warburg effect of cancer cells is to inhibit MCT1 by chemical compounds [57–60]. Because lactate is quite small, it was not obvious that a toxic molecule could be tagged onto a molecule passing the MCT1.

Our further investigations show that 18β-GA relies on MCT1 to be transported into cancer cells and higher expression of MCT1 made cells more susceptible to 18β-GA, thus suggesting that molecules considerably larger than lactate such as 18β-GA could be transported through MCT1 and thus targeting cancer cells through Warburg effect, with implications for a new strategy for cancer treatment.

2. Materials and methods

2.1. Cell culture reagents and antibodies

H1975 and A375 cell lines were gifts from Dr. Wensheng Wei at Peking University. A375 cells were cultured in Dulbecco's minimum eagle medium (DMEM). H1975 cells were cultured in Roswell Park Memorial Institute (RPMI)1640 medium. All cells were supplemented with 10% fetal bovine serum (FBS), with 1% penicillin/streptomycin, cultured in a humidified incubator with 5% CO_2 at 37 °C.

DMEM, RPMI 1640, trypsin, and FBS were purchased from Life Technologies/Gibco Laboratories (Grand Island, NY, USA). Lipofectamine 3000 (Invitrogen). 18β-GA and AZD3965 were purchased from MedChemExpress (MCE) (Shanghai, China), dissolved in DMSO.

2.2. Cell viability assays

Cells were seeded in a 96-well plate at a density of 10^4 cells/well for overnight, then incubated with 18β-GA at indicated concentrations for 24 or 48 h (h). After treatment, CellTiter-Glo (Promega), CCK-8 (Abcam), and LDH Cytotoxicity Assay Kit (Beyotime) were used to measure the percentage of cell death for each concentration compared to DMSO-treated cells.

2.3. Lentivirus packaging of plasmid library and infection

For lentivirus production, HEK293T cells were plated at approximately 40% confluence in five 10-cm dishes the day prior to transfection. On the day of transfection, a mixture containing 12 μg plasmid DNA (4 μg plasmid library: 4 μg psPAX2: 4 μg pMD2.G) was prepared in 500 μL pre-warmed Opti-MEM medium. This mixture was then combined with Lipofectamine 3000 in an additional 500 μL of Opti-MEM medium. After a 30-min incubation at room temperature, the transfection mixture was added drop-wise to the HEK293T cells. The viral supernatant was harvested 48 h post-transfection, filtered through a 0.45 μm Acrodisc syringe filter, aliquoted, and stored at −80 °C for future use. To determine the multiplicity of infection (MOI), target cells were seeded at 5×10^6 cells per well in six-well plates and infected with varying volumes of the viral supernatant supplemented with 8 μg/ml polybrene (Millipore, #TR-1003-G) in fresh medium for 24 h. Subsequently, the infected cells were transferred to 15-cm dishes and selected with puromycin (2 μg/mL).

2.4. Genome-scale CRISPR/Cas9 screening

The lentiviral gRNA plasmid library for genome-wide CRISPR-Cas9 screen was a gift from Dr. Wensheng Wei at Peking University. A total of 4×10^7 cells (MOI = 3) were plated on 10-cm dishes for sgRNA library construction. Cells were infected with the library and treated with 2 μg/mL of puromycin for 72 h post infection. SgRNA-iBAR-integrated cells were cultured for an additional 15 days to maximize gene knockout. Cells were re-seeded onto 10-cm dishes, treated by 18β-GA (130 μM) for 48 h, and followed by the removal of the loosely attached round cells through repeated pipetting. For each round of screening, cells were cultured in fresh media without 18β-GA to reach ~50–60% confluence. All resistant cells were pooled and subjected to another round of 18β-GA screening. For two subsequent rounds of screening, the 18β-GA concentration was 140 μM, and 150 μM, respectively. After three rounds of treatment, resistant cells and untreated cells were collected for genomic DNA extraction (QIAGEN, 69506), PCR amplification of sgRNA (KAPA, KK2625), and next genome sequencing (NGS).

To process the NGS data obtained from the screens, we employed the MAGeCK-iBAR algorithm [61], to assess the variation in sgRNA levels between control and experimental groups. Utilizing the standard settings within MAGeCK-iBAR, we determined the Robust Rank Aggregation (RRA) scores and p-values for each gene, taking into account the statistical significance and the replicability of the results across three iBARs.

2.5. Validation of candidate candidates

To validate each gene, we chose two sgRNAs designed in the library and cloned them into a lentiviral vector with a puromycin selection marker. We transfected the sgRNA plasmids into HEK293T cells with two lentiviral package plasmids (psPAX2 and pMD2.G). H1975 cells stably expressing Cas9 were infected with the lentivirus for 3 days and treated with 2 μg/mL puromycin for 2 days. 10^4 cells were seeded in 96-well plates, and three replicate wells were set up for each group. After 24 h, experimental groups were treated with 18β-GA, and control groups were treated with DMSO for 24-48 h. CCK-8 staining and detection were performed following the standard protocol. Experimental wells treated with 18β-GA were normalized to control wells.

2.6. Real-time qPCR

Cultured cells were treated with Trizol. RNA was extracted using the Direct-zol RNA kit (Zymo, R2069), and cDNA was synthesized using HiScript II 1st Strand cDNA Synthesis Kit (Vazyme, R21101). Real-time PCR was performed using ChamQ SYBR qPCR Master Mix (Vazyme, R211-01) on LightCycler96 qPCR system (Roche). Relative mRNA level was calculated using the $2^{(-\Delta\Delta CT)}$ method. Actin was used as an internal control. All the primers used for real-time qPCR are listed in Table S2 in Supporting Information.

2.7. Immunofluorescence

Cells were seeded in PDL coated glass-bottomed dish for 24 h. After cells were attached to the bottom, old media were replaced with 4% PFA and fixed for 10 min at RT before being washed in phosphate buffered saline Triton (PBST, PBS containing 0.2% Triton X-100, vol/vol) for 5 min three times, blocked in 500 μL PB buffer (PBS containing 2% Triton X-100, 10% normal goat serum, vol/vol) for 30 min. Expression of MCT1 was detected by cell incubation with primary antibodies in the dilution buffer (PBS containing 0.25% Triton X-100, 1% normal goat serum, vol/vol) for 12 h at 4 °C, followed by being washed with the washing buffer (PBS containing 1% Triton X-100, vol/vol, 3% NaCl, g/ml) three times, each for 10 min. Cells were incubated with secondary antibodies in the dilution buffer for 1 h at RT in darkness and washed three times in the washing buffer for 10 min each. Finally, cells were

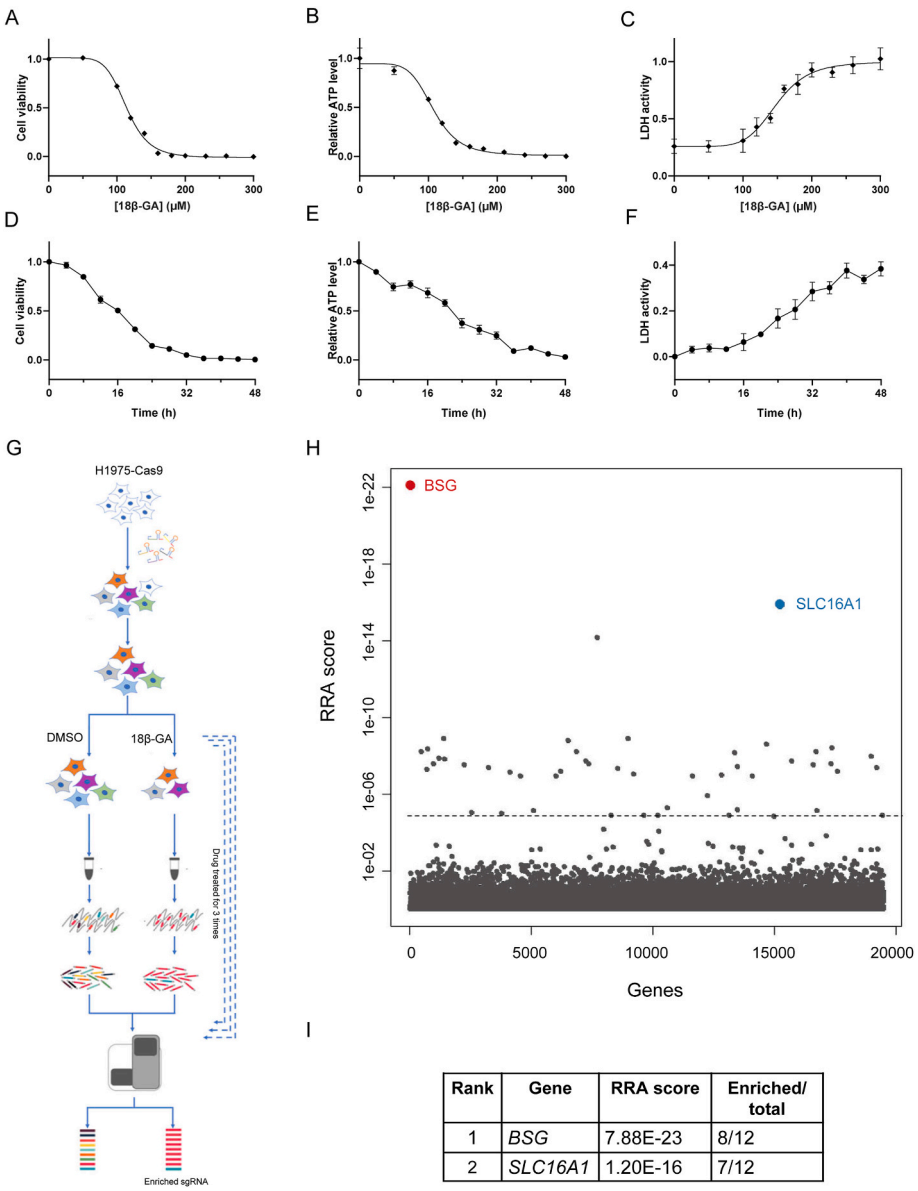

Rank	Gene	RRA score	Enriched/ total
1	*BSG*	7.88E-23	8/12
2	*SLC16A1*	1.20E-16	7/12

Fig. 1. Whole-genome CRISPR screening for genes required for 18β-GA sensitivity. (*A-C*) Dose-dependent effects of 18β-GA on H1975 cells after 48 h treatment: cell viability (*A*), ATP level (*B*) and LDH activity (*C*), with DMSO used as the control. (*D-F*) Time-dependence of the effects of 160 μM 18β-GA on H1975 cells. (*G*) A schematic diagram of the CRISPR screen for genes required for 18β-GA sensitivity in H1975 cells. (*H*) Robust rank aggregation (RRA) scores of all genes from the screen. (*I*) Gene hits from the screen. The top 2 hits are *SLC16A1* and *BSG*. RRA score-based ranking, RRA score, and the number of sgRNA enriched in screening are listed. Data are represented as means ± standard deviation (SD), n = 3 for panels *A-F*.

imaged on a Zeiss LSM880 confocal microscope.

A rabbit anti-MCT1 antibody (1:500 dilution; Santa Cruz, catalog no. sc-365501) was used, and the secondary antibody was Alexa Fluor488 anti-rabbit immunoglobulin G (1:2000 dilution; Life Technology, catalog no. A11034).

2.8. Correlation analysis

Seventeen cell lines (H1299, H2452, U2OS, TCCSUP, UM-UC-3, H1975, RKO, PC-3, HCT-15, TE-1, DU-145, COLO-680 N, H226, HCT-116, H522, A375 and MSTO-211H) were treated with 18β-GA (0-200 μM). After 48 h, cell viability was quantified via CCK-8 assay, and EC_{50} values were interpolated from the resulting dose-response curve using a nonlinear regression model. *SLC16A1* mRNA level was detected by qPCR. Transcriptome-wide normalized mRNA levels from gene expression profiling experiments were obtained from CCLE [62] for all 17 cell lines. The mRNA expression pattern across all 17 samples for each of the genes was then correlated with the EC_{50} values.

2.9. Liquid chromatography-tandem mass spectrometry assay

Uptake assays were performed by plating cells in six-well plates (8×10^5 cells per well) the day before experiments. Cells were treated with 18β-GA for up to 8 h at 37 °C before being washed three times with ice-cold PBS and lysed in 100-1000 μl of 80% ice-cold methanol. After centrifugation at 4 °C, 16,000g for 10 min, supernatants were dried with a nitrogen evaporator and reconstituted in 1 ml 50% ACN (Acetonitrile). The concentrated samples were analyzed by LC-MS/MS (ThermoFisher Vanquish HPLC coupled to a ThermoFisher TSQ Altis Triple Quadrupole Mass Spectrometer). LC-MS detected and analysis was performed by the CIBR mass spectrometry core facility.

Chromatographic separations were carried out with a ThermoFisher Vanquish HPLC, 1.9 μm, 2.1 × 100 mm analytical column. The column was maintained at 40 °C and 5 μL samples were injected per run. Mobile

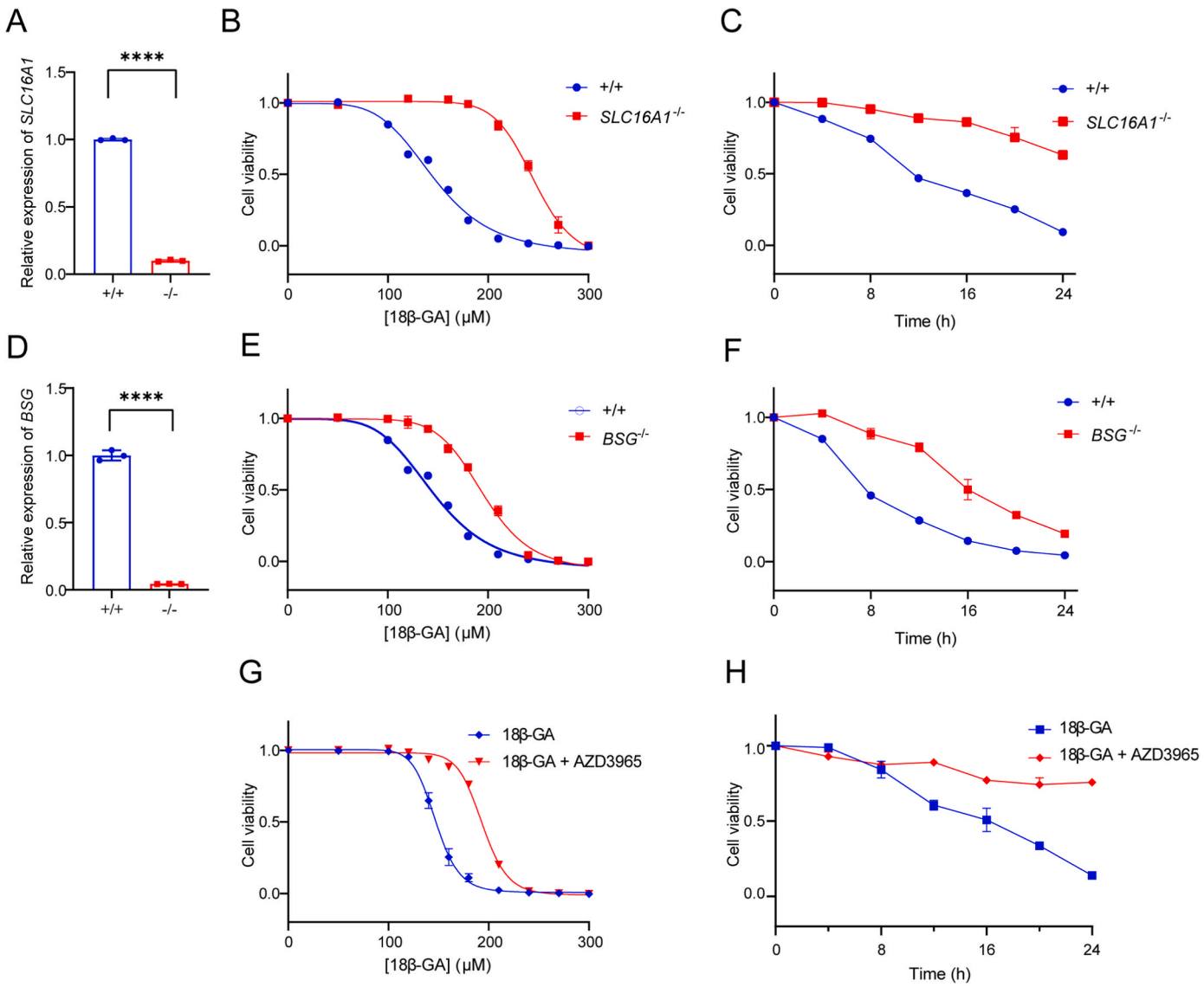

Fig. 2. Validation of candidate genes identified from the screen. (*A*) *SLC16A1* mRNA levels detected in WT and *SLC16A1*$^{-/-}$ H1975 cells by qPCR. Two-tailed unpaired Student's *t*-test was used (****P < 0.001). (*B* and *C*) Effects of *SLC16A1* knockout on 18β-GA-induced cell death. Cell viability in WT and *SLC16A1*$^{-/-}$ H1975 cells are shown following treatment with indicated concentrations of 18β-GA for 24 h (*B*) and treatment with a 160 μM concentration for indicated durations (*C*). (*D*) *BSG* mRNA levels detected in WT and/*BSG*$^{-/-}$ H1975 cells. (*E* and *F*) Effects of *BSG* knockout on 18β-GA-induced cell death. Cell viability in WT and *BSG*$^{-/-}$ H1975 cells are shown following 18β-GA treatment under the same conditions as in panels (*B*) and (*C*). (*G* and *H*) Effects of MCT1 inhibitors on 18β-GA-induced cell death. Cell viability in H1975 cells in the absence or presence of the MCT1 inhibitor AZD3965 (10 nM) followed by 18β-GA treatment under the same conditions as in panels (*B*) and (*C*). Data are represented as means ± SD, n = 3 for all panels.

phase A was 5 mM ammonium acetate (pH = 7) and mobile phase B was ACN. For analysis of 18β-GA, gradient elution was applied by increasing mobile phase B from 5% to 95% within 7 min; the total analysis time was 12 min with the flow rate set to 0.3 mL min^{-1}. The compounds were detected in a negative electrospray ionization mode. The multiple reaction monitoring transition 469 → 425.3. A six-point calibration curve was determined to allow quantification.

2.10. Statistics

All statistical analyses were carried out with Prism 5 (GraphPad Software). Mann-Whitney tests were used to compare two columns of data. One-way analysis of variance (ANOVA) followed by Tukey's multiple comparison posttest was used to compare multiple columns of data. Statistical significance is denoted by asterisks: * = p < 0.05, ** = p < 0.01, *** = p < 0.001, **** = p < 0.0001.

4. Results

4.1. CRISPR-based whole-genome screening for genes required for 18β-GA sensitivity

We examined the toxic activity of 18β-GA on human non-small cell lung cancer cells H1975. 18β-GA reduced H1975 cell viability with a half-maximal effective concentration (EC_{50}) of 112.3 μM, consistent with previous observations in other cell lines [14]. Measurement of extracellular lactate dehydrogenase (LDH) and intracellular adenosine triphosphate (ATP) levels showed that 18β-GA induced H1975 cell death in a dose-dependent (Fig. 1A–C) and time-dependent manner (Fig. 1D–F).

To find genes involved in 18β-GA-induced cancer cell death, we utilized a CRISPR/Cas9 high-throughput screening to conduct a genome-wide selection of targets associated with 18β-GA-induced cell death [26–30]. The human whole-genome small guide ribonucleic acid

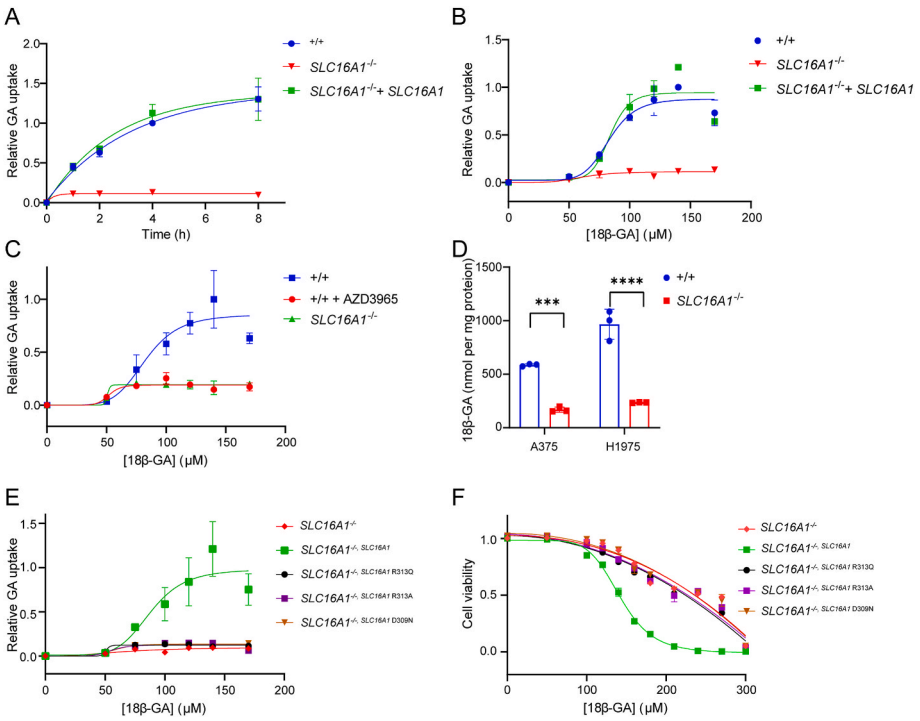

Fig. 3. Requirement of MCT1 for the transport of 18β-GA into the cell. (*A*) Intracellular 18β-GA levels in WT, *SLC16A1*$^{-/-}$, and *SLC16A1*$^{-/-,SLC16A1}$ H1975 cells following 140 μM 18β-GA incubation, measured by MS over time. Each relative 18β-GA uptake was normalized to WT H1975 cells treated with 140 μM 18β-GA for 4 h. (*B*) Dose curves of intracellular 18β-GA content in WT, *SLC16A1*$^{-/-}$, and *SLC16A1*$^{-/-,\ SLC16A1}$ H1975 cells following 4 h of 18β-GA incubation. (*C*) MCT1 inhibitor diminished the 18β-GA uptake in WT H1975 cells. Dose curves of intracellular 18β-GA levels in the absence or presence of 10 nM AZD3965. (*D*) 18β-GA uptake in WT A375 or H1975 and *SLC16A1*$^{-/-}$ A375 or H1975 cells. Two-tailed unpaired Student's t tests were used (****P < 0.0001, ***P < 0.001). (*E*) Effects of *SLC16A1* lactate-binding site mutations on 18β-GA transport activities. 18β-GA uptake in *SLC16A1*$^{-/-}$ H1975 cells re-expressing *SLC16A1* WT, *SLC16A1* R313Q, *SLC16A1* R313A, or *SLC16A1* D309 N after 4-h incubation with 18β-GA. (*F*) Effects of *SLC16A1* lactate-binding site mutations on 18β-GA sensitivities. Cell viability after 24 h of 18β-GA treatment in mutant cell lines. Data are represented as means ± SD, n = 3 for all panels.

(sgRNA) library used here targets 19,114 genes with a total of 233,000 sgRNAs [61]. The sgRNA library was constructed with three internal barcodes (iBARs), which ensures a high-quality screening even at a high multiplicity of infection (MOI) while significantly reducing the number of cells required for the screening process. We stably infected this CRISPR sgRNA library into the H1975 cell line stably expressing Cas9. Following the construction of the cell library, it was evenly divided into two groups. One group served as the experimental group, which was treated with 18β-GA to enrich cells resistant to 18β-GA. The other group served as the control group, which was treated with an equivalent concentration of DMSO. After three rounds of chemical treatment, we isolated genomic DNA from the enriched cells from the experimental group and the control group cells. The sgRNA region was PCR-amplified and sequenced with next-generation sequencing (Fig. 1G).

The distribution of sgRNA distribution in the experimental group of cells was compared with that of the control group to calculate differences in sgRNA abundance. By integrating the results from three rounds of drug treatment, genes corresponding to the most enriched sgRNAs in the experimental group were identified using the MAGeCK-iBAR algorithm [61]. The screening results showed the top two genes to be *SLC16A1* and *BSG* (Fig. 1H and S1). Robust rank aggregation (RRA) scores and false discovery rate (FDR) values for these two genes were highly significant (Fig. 1I). The gene *SLC16A1* encodes MCT1, which is a proton-coupled monocarboxylate transporter for monocarboxylic acids including lactate and pyruvate across the cell membrane [37–41]. The gene *BSG* encodes basigin, a chaperone molecule essential for escorting MCT1 to the plasma membrane [46,47].

4.2. Validation of SLC16A1 and BSG in 18β-GA sensitivity

To validate the role of these two genes, we selected two sgRNAs for each gene (Table S1). We isolated two clonal H1975 cell lines in which *SLC16A1* and *BSG* mRNA were targeted and confirmed by quantitative polymerase chain reaction (qPCR) (Fig. 2, A and D). Knocking out *SLC16A1* did not alter *BSG* expression, and vice versa (Fig. S2). Consistent with the screening results, the viability of control cells was decreased by increasing concentrations of 18β-GA for 24 h, whereas the viability of cells lacking *SLC16A1* was significantly increased under the same conditions (Fig. 2B). The viability of cells was also decreased by a fixed concentration of 18β-GA at different time points, an effect significantly reversed by genetic targeting of *SLC16A1* (Fig. 2C). Genetic targeting of *BSG* also decreased the sensitivity of H1975 cancer cells to 18β-GA, as assayed by either concentration-dependence (Fig. 2E) or time-dependence (Fig. 2F). We also used an MCT1 specific chemical inhibitor, AZD3965 [65–72]. 18β-GA-induced H1975 cell death was significantly reduced by AZD3965 (Fig. 2G and H). Together, genetic and pharmacological results confirm CRISPR-based screening outcomes and demonstrate that *SLC16A1* and *BSG* are required for induction of cell death by 18β-GA.

4.3. Requirement of MCT1 for cellular uptake of 18β-GA

We investigated the mechanism by which MCT1 functioned in 18β-GA-induced cell death. Previous findings of MCT1 facilitated transport of drugs [73,74] promoted us to test whether MCT1 could facilitate the cellular uptake of 18β-GA.

We incubated wild-type (WT) and knockout H1975 cells with 18β-GA before repeatedly washing the cells to remove 18β-GA adhering to the cell surface and measuring the intracellular content of 18β-GA by mass spectrometry. The intracellular 18β-GA levels of H1975 WT cells were increased in a time dependent manner (Fig. 3A). It was also increased in a concentration-dependent manner after 4-h exposure to

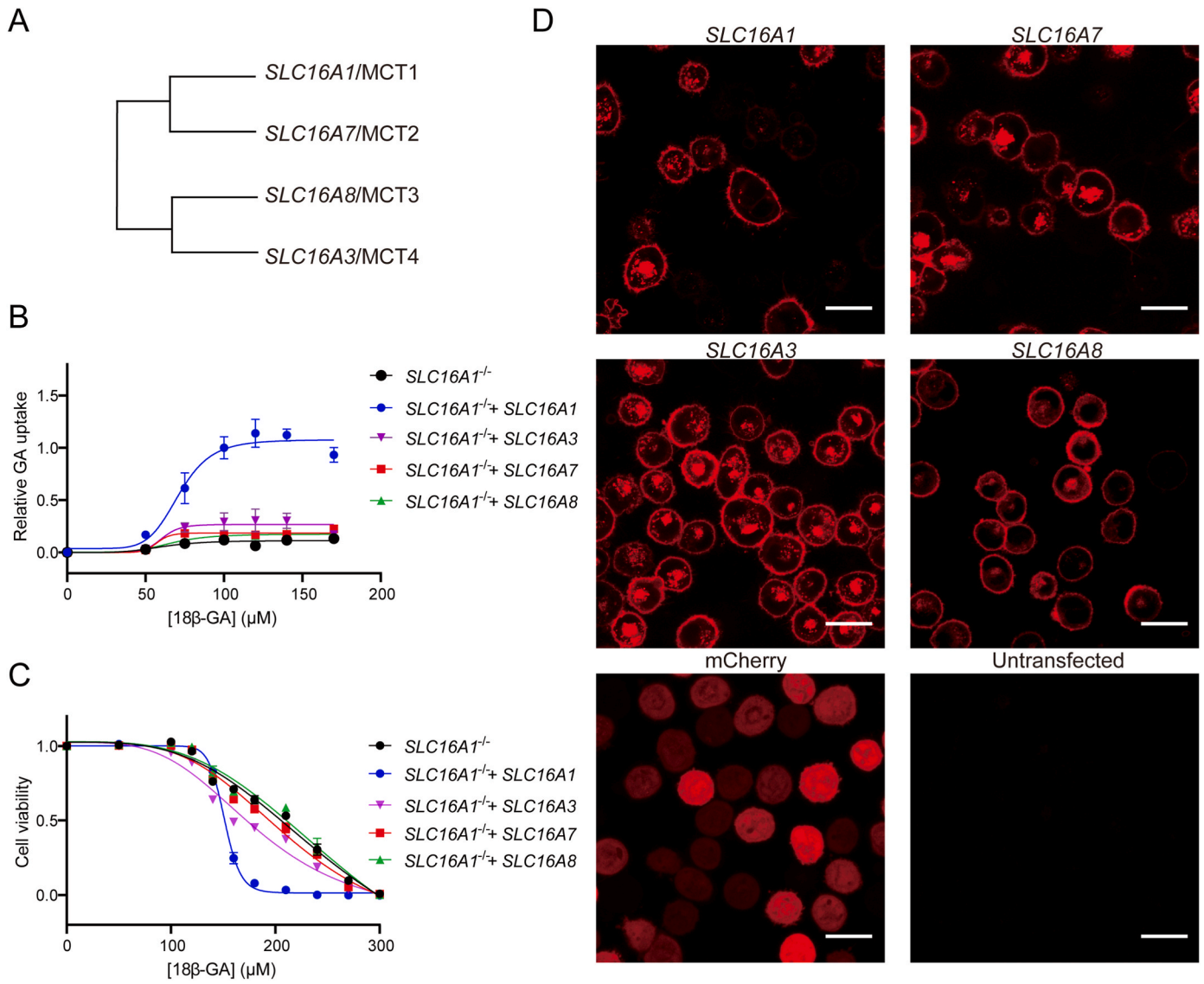

Fig. 4. Failure of MCT 2-4 expression to restore 18β-GA cellular uptake and sensitivity. (*A*) A phylogenetic tree of the SLC16 subfamily. ClustalW alignment was carried out to generate the phylogenetic tree by using the 'Neighbor Joining' method. (*B*) 18β-GA transport activities of the SLC16 family. 18β-GA uptake in *SLC16A1*$^{-/-}$ H1975 cells reexpressing *SLC16A1*, *SLC16A3*, *SLC16A7*, and *SLC16A8*-mCherry after 4-h incubation with 18β-GA. (*C*) Cell viability following treatment with 18β-GA in cells expressing different members of the SLC16 family. (*D*) Membrane localization of SLC16 family members expressed in *SLC16A1*$^{-/-}$ H1975 cells. Scale bar, 30 μm. Data are represented as means ± SD, n = 3 for all panels.

18β-GA (Fig. 3B). Genetic targeting of *SLC16A1* in H1975 cells significantly reduced the intracellular content of 18β-GA, as supported both by the time- (Fig. 3A) and dose-dependent curves (Fig. 3B). This result was further confirmed in a different cell line (A375 melanoma cells; Fig. 3D).

To confirm that the phenotype of *SLC16A1*$^{-/-}$ mutant clones was indeed caused by the lack of the *SLC16A1* gene, we introduced exogenous *SLC16A1* into the *SLC16A1*$^{-/-}$ cells (as confirmed by qPCR; Fig. S3A). We found that exogenous *SLC16A1* could rescue the 18β-GA uptake phenotype of H1975 cells, as both indicated the time- (Fig. 3A) and dose-dependent curves (Fig. 3B). Thus, MCT1 is necessary and sufficient for cellular uptake of 18β-GA.

This was further confirmed by examining whether the MCT1 specific inhibitor, AZD3965 could affect the transport of 18β-GA. Our results showed that AZD3965 significantly reduced the intracellular content of 18β-GA, with an inhibition level close to that observed in the knockout cell lines (Fig. 3C). Thus, both the genetic and the pharmacological support that MCT1 is essential for 18β-GA transport.

Amino acid residues arginine at position 313 (R313) and aspartate at 309 (D309) of MCT1 were reportedly involved in its binding to lactate, and the same mutations have been shown to abrogate lactate transport [71]. We therefore introduced these previously validated mutations (R313A/Q, D309 N) into MCT1, and expressed them in *SLC16A1*$^{-/-}$ cells. qPCR results confirmed MCT1 expression (Fig. S3B). MCT1 protein with any of these mutations (R313Q, R313A, or D309 N) could not transport 18β-GA (Fig. 3E). H1975 cells expressing any of these mutants could not restore sensitivity of *SLC16A1*$^{-/-}$ cells to 18β-GA (Fig. 3F).

4.4. Failure of other MCTs in cellular uptake of and cell death induction by 18β-GA

MCT1 belongs to the SLC16 family, and among the 14 MCTs, MCT1-MCT4 mediate the proton-coupled influx or efflux of monocarboxylic acids (Fig. 4A), with the direction of transport determined by the concentration gradients of protons and monocarboxylate anions [33,34,36,75]. Because their substrate specificities were different, we investigated whether MCTs 2, 3 or 4 could function similarly as MCT1 in transporting 18β-GA.

We introduced MCT 2 (*SLC16A7*), 3 (*SLC16A8*) or 4 (*SLC16A3*)

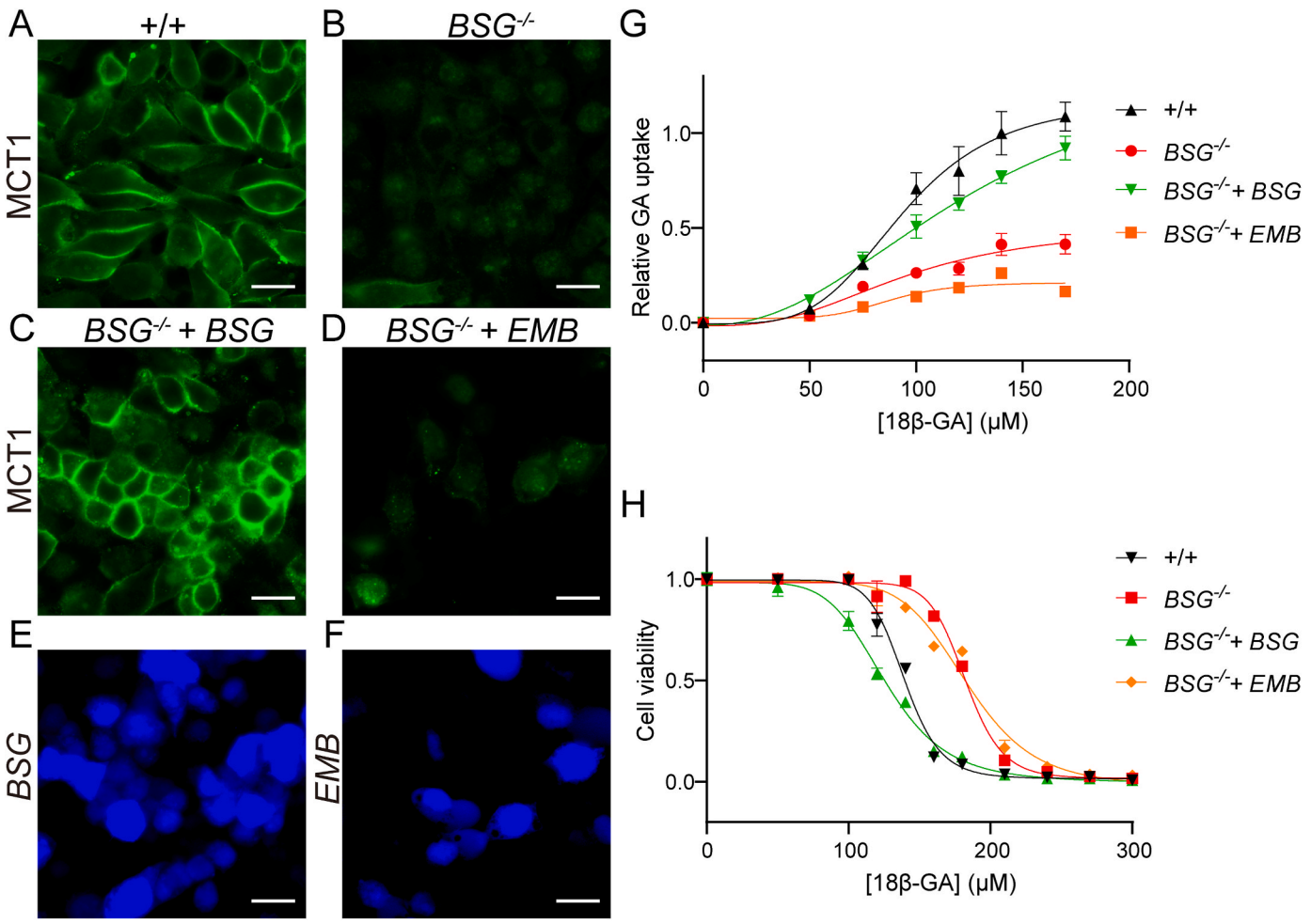

Fig. 5. Membrane localization of MCT1 facilitated specifically by BSG to enable 18β-GA uptake and cytotoxicity. (*A* and *B*) Immunofluorescence results showing the subcellular localization of MCT1 in WT and *BSG*$^{-/-}$ A375 cells. (*C–F*) Subcellular localization of MCT1 after EMB/BSG-P2A-BFP expression in *BSG*$^{-/-}$ A375 cells. BFP indicates the expression of the indicated genes. Scale bar, 30 μm. (*G*) 18β-GA uptake in WT, *BSG*$^{-/-}$, *BSG*$^{-/-,\ BSG}$, *BSG*$^{-/-,\ EMB}$ A375 cells. (*H*) Cell viability after 18β-GA treatment of in WT, *BSG*$^{-/-}$, *BSG*$^{-/-,\ BSG}$, *BSG*$^{-/-,\ EMB}$ A375 cells. Data are represented as means ± SD, n = 3 for all panels.

individually into the H1975 clone lacking MCT1 (*SLC16A1*$^{-/-}$), with the qPCR results confirming their expression (Fig. S4). We further confirmed that MCT 2, 3 and 4 proteins were located on the plasma membrane (Fig. 4D). After incubating H1975 cells with 18β-GA, we assessed cell viability and cellular uptake of 18β-GA. Only exogenous MCT1, but not MCT 2, 3 or 4 could restore 18β-GA uptake into H1975 cells lacking endogenous MCT1 (Fig. 4B). Similarly, cell death induction by 18β-GA could only be restored to H1975 cells lacking endogenous MCT1 by expression of exogenous MCT1 but not by MCT 2, 3 or 4 (Fig. 4C). Thus, MCT1 is specifically required for 18β-GA uptake into cells and induction of cell death.

4.5. *BSG as the cofactor for MCT1 required for 18β-GA transport and function*

BSG and Embigin (EMB) are two molecular chaperones previously reported to assist the translocation of MCT1-4 to the plasma membrane [36,47,73,76,77].

To examine the involvement of *BSG* in MCT1 membrane localization and subsequent impact on 18β-GA's effect on cell viability, we performed *BSG* knockout in melanoma cells A375 and assessed MCT1 subcellular localization using an anti-MCT1 antibody in both A375/*BSG*$^{-/-}$ and WT cells. MCT1 was localized on the cell membrane of WT A375 cells (Fig. 5A), but not on the cell membrane of *BSG*$^{-/-}$ A375 cells (Fig. 5B and Fig. S5C). 18β-GA uptake was reduced in *BSG*$^{-/-}$ cells (Fig. 5G) and cell death caused by 18β-GA treatment was enhanced in *BSG*$^{-/-}$ cells (Fig. 5H).

We then introduced *BSG* and *EMB* into the *BSG*$^{-/-}$ cell line, with qPCR results confirming their expression (Fig. S5, A and B). Only *BSG* expression rescued the phenotype of MCT1 membrane localization (Fig. 5C), whereas *EMB* did not (Fig. 5D). We also evaluated 18β-GA transport and sensitivity in these cells. Exogenous *BSG* expression into the *BSG*$^{-/-}$ cells showed a significant increase in 18β-GA transport activity, nearly to the WT level (Fig. 5G), and a marked increase in cell death response to 18β-GA (Fig. 5H). Exogenous *EMB* expression into the *BSG*$^{-/-}$ cells did not restore either cellular uptake of 18β-GA (Fig. 5G) or cell death response to 18β-GA (Fig. 5H).

Thus, BSG, but not EMB, is the key cofactor for MCT1 localization to the plasma membrane, which is essential for 18β-GA transport and of cell death.

4.6. *SLC16A1 expression, cancer prognosis and 18β-GA sensitivity*

To examine whether *SLC16A1* expression is associated with patient outcome, we analyzed the correlation between *SLC16A1* expression levels and patient prognosis of overall survival (OS) for all TCGA cases (Fig. 6A). Within individual tumor types, high *SLC16A1* expression was independently significantly associated with poor OS in low grade glioma (LGG) (logrank p = 6.20E-07, HR = 5.5, p(HR) = 8.80E-06) (Fig. 6B), lung adenocarcinoma (LUAD) (logrank p = 0.00022, HR = 2.3, p

A

	Logrankp	HR(high)	p(HR)
LGG	6.20E-07	5.5	8.80E-06
LUAD	0.00022	2.3	0.00031
PAAD	0.0016	2.8	0.0023
SARC	0.0033	2.7	0.0047
ACC	0.00071	15	0.01
BLCA	0.016	1.9	0.018
READ	0.03	0.2	0.048
KIRP	0.093	2.1	0.1
OV	0.11	0.73	0.1
CESC	0.13	1.8	0.13
UCS	0.14	2.4	0.15
SKCM	0.19	1.3	0.19
UVM	0.24	0.42	0.25
LAML	0.29	1.6	0.29
LUSC	0.37	0.82	0.37
HNSC	0.38	1.2	0.38
MESO	0.37	0.72	0.4
LIHC	0.48	1.2	0.48
BRCA	0.56	1.2	0.55
COAD	0.63	0.8	0.63
KIRC	0.69	1.1	0.69
TGCT	0.77	0.66	0.77
DLBC	0.79	1.3	0.79
GBM	0.78	0.94	0.82
ESCA	0.84	1.1	0.84
CHOL	0.84	0.85	0.84
UCEC	0.92	0.95	0.92
STAD	0.93	0.98	0.94
PRAD	0.99	0.98	0.99
KICH	0.0023	2.80E+09	1
THCA	0.035	5.40E+08	1
PCPG	0.17	5.60E+08	1
THYM	0.34	6.70E-10	1

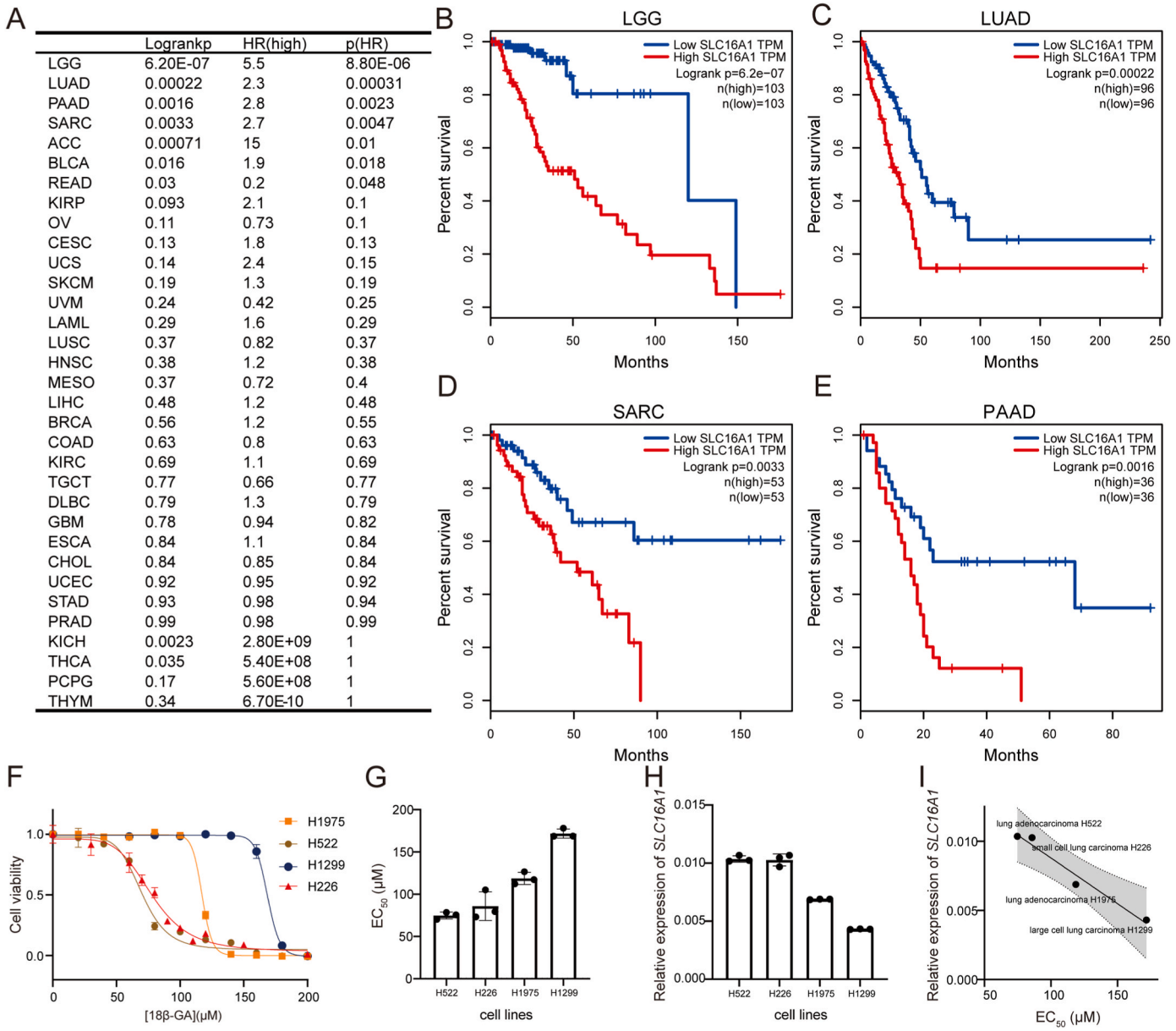

Fig. 6. Correlation of higher MCT1 expression correlates with poorer LUAD patient survival and higher 18β-GA sensitivity. (*A*) Kaplan-Meier analysis of overall survival (OS) based on *SLC16A1* expression in the TCGA pan-cancer cohort (low, <20%; high, >80%) using the GEPIA platform. The Log-rank test (Mantel-Cox test) was applied to compare overall survival (OS) between groups. Cox proportional hazards regression analysis provided the hazard ratio and p-value. Data sourced from The Cancer Genome Atlas (TCGA). (*B*) Kaplan-Meier survival analysis for tumor types with significant contribution of *SLC16A1* to survival (low, <20%; high, >80%). LGG, Brain Lower Grade Glioma; LUAD, Lung adenocarcinoma; SARC, Sarcoma; PAAD, Pancreatic adenocarcinoma. The P-value is from the log-rank test. (*C*) Cell viability of four lung carcinoma cell lines after indicated concentrations of 18β-GA treatment for 48 h. (*D*) Calculated EC_{50} values from panel (*C*). (*E*) *SLC16A1* mRNA levels by qPCR. (*F*) Correlation between *SLC16A1* expression levels and cell sensitivity to 18β-GA (EC_{50}). Data are represented as means ± SD, n = 3 for all panels.

(HR) = 0.00031) (Fig. 6C), soft tissue carcinoma (SARC) (logrank p = 0.0033, HR = 2.7, p(HR) = 0.0047) (Fig. 6D) and pancreatic adenocarcinoma (PAAD) (logrank p = 0.0016, HR = 2.8, p (HR) = 0.0023) (Fig. 6E). While these results add *SLC16A1* as one of the molecular markers in the prognosis diagnosis, our findings above suggest the new possibility that they would be more sensitive to drugs such as 18β-GA which targets MCT1 for entry into and killing of cancer cells.

LUAD is one of the malignant tumors with the highest mortality rate globally (accounting for approximately 45% of lung cancer cases) [78] and a five-year survival rate of less than 20% [79]. We used four human lung carcinoma cell lines (H226, H1299, H522, and H1975) to evaluate the therapeutic potential of 18β-GA. Dose-dependent cellular responses were assessed in a concentration range of 0-200 μM (Fig. 6F). The half-maximal effective concentration (EC_{50}) was calculated using nonlinear regression analysis (four-parameter logistic model) (Fig. 6G). Quantitative real-time PCR was performed to quantify *SLC16A1* mRNA expression levels (Fig. 6H), for correlation analysis with 18β-GA sensitivity.

A significant inverse correlation between *SLC16A1* expression and 18β-GA resistance was observed (Fig. 6I): lung carcinoma cell lines with higher *SLC16A1* mRNA levels (H522 and H226) exhibited greater sensitivity to 18β-GA (EC_{50} = 74.78 μM) compared to low-expressing lines (H1299: EC_{50} = 171.8 μM; $P < 0.01$, Pearson's $r^2 = 0.9678$).

Thus, in addition to the expectation of MCT1 allowing better cancer cell survival and worse patient survival, our finding of MCT1 in 18β-GA sensitivity suggests a new opportunity that MCT1 is a biomarker for 18β-GA-based cancer therapies.

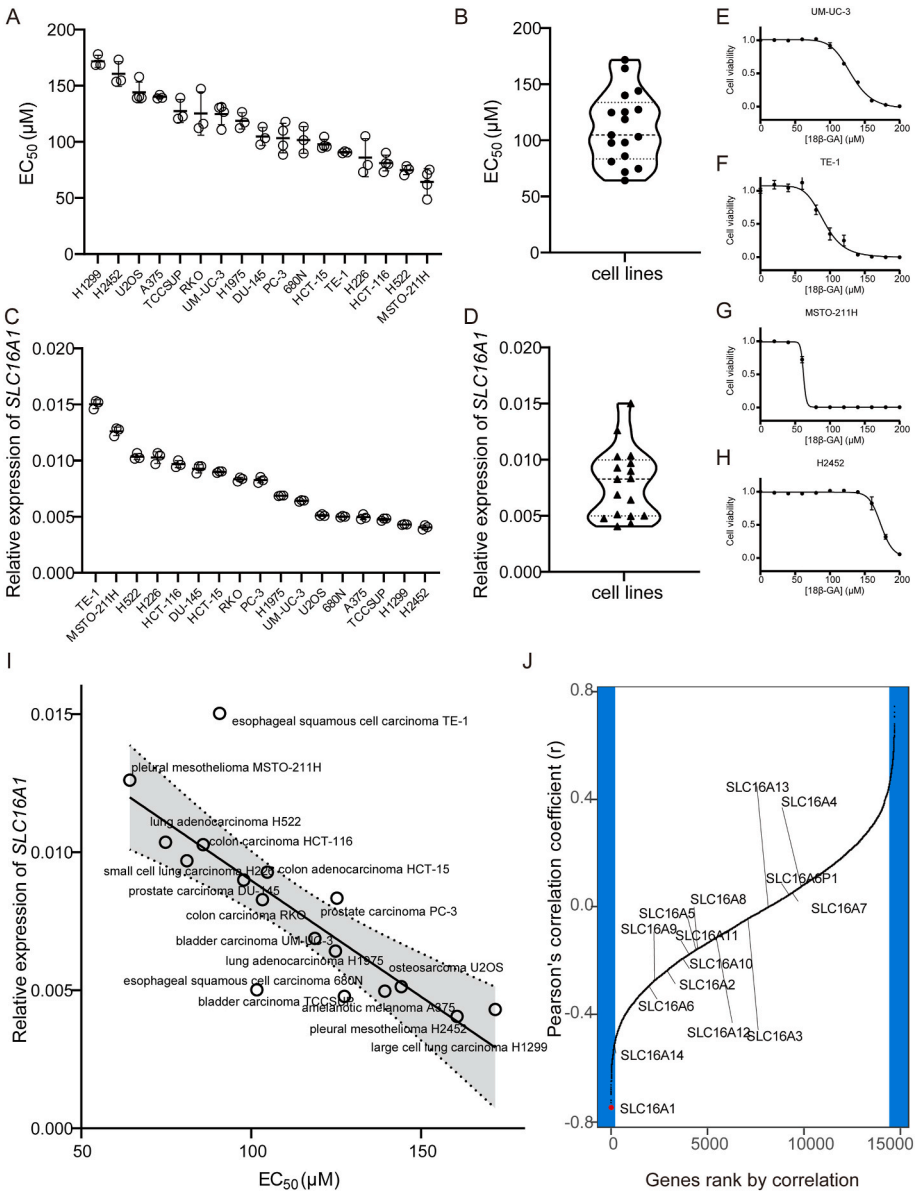

Fig. 7. MCT1 expression as the predominant determinant of cancer cell sensitivity to 18β-GA. (*A*) EC_{50} values for 18β-GA treatment of cancer cells, calculated from the dose response curves shown in Fig. S6 and (E-H). (*B*) Violin plot of EC_{50} values from panel (*A*). (*C*) Expression levels of *SLC16A1* in cancer cells determined by qPCR. (*D*) Violin plot of *SLC16A1* expression levels from panel (*C*). (*E-H*) Cell viability of UM-UC-3, TE-1, MSTO-211H, H2452 after 18β-GA treatment for 48 h. Other cell lines are shown in Fig. S6. (*I*) Correlation between *SLC16A1* expression levels and cell sensitivity to 18β-GA EC_{50}. (*J*) Pearson correlation coefficients of EC_{50} values with gene expression levels in the CCLE database. *SLC16* family transporter genes were labeled, and *SLC16A1* is represented by red dots. Data are represented as means ± SD, n = 3 for all panels. (For interpretation of the references to colour in this figure legend, the reader is referred to the Web version of this article.)

4.7. MCT1 expression predictive of 18β-GA sensitivity in cancer cells

To study the relevance of *SLC16A1* as a predictive biomarker other than LUAD, we expanded our analysis to a panel of 17 cell lines spanning eight cancer types (prostate, colon, esophageal, lung, bladder, amelanotic melanoma, pleural mesothelioma, osteosarcoma). Despite their diverse origins, they exhibited a robust inverse correlation between *SLC16A1* mRNA levels and 18β-GA sensitivity (Pearson's r = −0.8006, P = 0.0002; Fig. 7A–I and Fig. S6).

Because there are other MCTs in the human genome, we performed an unbiased analysis of whether the expression level of *SLC16A1* is the most significant gene conferring 18β-GA sensitivity. We analyzed the whole gene expression levels of these cell lines in the Cancer Cell Line Encyclopedia (CCLE) database [62] and performed a correlation analysis with EC_{50}. Our results show that among 20,000 genes, the mRNA level of *SLC16A1* has the highest correlation with the EC_{50} of cell sensitivity to 18β-GA (Fig. 7J).

By contrast, the expression levels of other MCTs were not significantly correlated with the EC_{50} of 18β-GA sensitivity (Fig. 7J and Fig. S7).

These results indicate that the levels of *SLC16A1* gene expression are the best genetic predictor of 18β-GA sensitivity, suggesting that, while Warburg effect requires higher lactate transport for cancer cell survival and higher MCT1 predicts worse prognosis, higher MCT1 can also be targeted by drugs such as 18β-GA which enters cancer cells to kill them.

5. Discussion

We have performed a genome-wide CRISPR screen to identify genes required for 18β-GA sensitivity, a molecule from a Chinese medicinal

herb known to have anticancer activities. We found the lactate transporter, MCT1, and its membrane chaperone BSG, as major determinants of 18β-GA sensitivity. MCT1 plays a pivotal role in cellular uptake of 18β-GA, while BSG is required for MCT1 localization to the plasma membrane. *SLC16A1* mRNA levels predict 18β-GA sensitivities of human cancer cells. Our study demonstrates a direct link between *SLC16A1*-mediated 18β-GA transport and its cytotoxic effects on cancer cells.

Our analysis of TCGA data uncovers a significant correlation between high *SLC16A1* expression and poor prognosis in multiple cancer types, which is noteworthy given the recent interest in the development of personalized medicine strategies based on the molecular characteristics of tumors. This correlation can be turned upside down if drugs such as 18β-GA are used to enter cancer cells via MCT1. Our experiments with cancer cell lines support this suggestion and further substantiate the role of *SLC16A1* in 18β-GA transport. The correlation between *SLC16A1* expression levels and EC_{50} for 18β-GA values of cell lines from the CCLE database confirms *SLC16A1* as a significant predictor of 18β-GA sensitivity. However, under in vitro experimental conditions, 18β-GA requires a high concentration to kill tumor cells. Therefore, the molecular structure of 18β-GA should be modified so that the concentration required to kill cells is reduced and the potency is increased; at the same time, the ability to be transported by *SLC16A1* is retained, which can have the effect of treating tumors with high expression of *SLC16A1*. Such compounds hold promise for new drugs targeting tumors with the Warburg effect.

MCT1 has been a known target for cancer treatment, but it has been targeted by small molecule inhibitors [65–72], which inhibit lactate export from cancer cells, causing cell death. 18β-GA is different in that it utilizes MCT1 to enter the cell before exerting toxic effects.

Drugs going through transporters have been known but are not cancer specific. SLCs for the cellular uptake of chemical molecules are important. For example, the nucleotide transporter SLC29A1 is linked to the transport of nucleoside analog drugs such as clofarabine, gemcitabine, and fluorouracil [80]. The folate transporter SLC19A1 transports methotrexate and pemetrexed [81,82] and the organic cation transporter SLC22A1 (OCT1) has been reported to be associated with metformin transport [83,84]. The U.S. Food and Drug Administration and the European Medicines Agency currently advocate for the testing of ABC and SLC22/SLCO family members in clinical drug interaction studies [85]. Screening of a CRISPR-Cas9 KO library for SLC, targeting 394 human SLC genes and 60 cytotoxic drugs has shown a large number of SLC-compound associations, including *SLC11A2/SLC16A1* with artemisinin derivatives and *SLC35A2/SLC38A5* with cisplatin [86]. This approach may also lead to the identification of more small molecules derived from natural products, such as those extracted from herbs, for potential therapeutic use.

Because 18β-GA is not highly toxic, an obvious suggestion is to make derivatives more potent in killing cancer cells but retain its property of entering cells via MCT1-whose substrate pocket may recognize the monocarboxylate of 18β-GA through the same Arg313 and Asp309 residues used for lactate binding. Drugs should be modified from 18β-GA to enter cancer cells via MCT1 but are more toxic than 18β-GA. Drugs can also be structurally different from 18β-GA but use the same mechanism: entering cancer cells via MCT1 and causing cell death.

Funding declaration statement

This research did not receive any specific grant from funding agencies in the public, commercial, or not-for-profit sectors.

CRediT authorship contribution statement

Bingxin Xia: Conceptualization, Data curation, Formal analysis, Investigation, Methodology, Project administration, Resources, Software, Supervision, Validation, Visualization, Writing – original draft. **Chen Zhu:** Methodology, Writing – review & editing. **Yi Rao:** Conceptualization, Writing – review & editing.

Declaration of competing interest

The author declares no conflicts of interest with the contents of this article.

Acknowledgments

We are grateful to Dr. Wensheng Wei from Peking University for offering the CRISPR library plasmids and cell lines expressing Cas9. We are grateful to Drs. Eric Erquan Zhang and Guotai Xu from the National Institute of Biological Sciences, Beijing (NIBS), Peng Du, Zhengfan Jiang and Zexian Zeng from Peking University for kindly providing the cancer cell lines. We are grateful to the Biological Mass Spectrometry Center at CIBR and Ms. Xiangli Sun and Ms. Xiaoqian Yu for assistance with LC-MS analyses.

Appendix A. Supplementary data

Supplementary data to this article can be found online at https://doi.org/10.1016/j.bbrc.2026.153492.

Data availability

The raw sequence data reported in this paper have been deposited in the Genome Sequence Archive [63] in National Genomics Data Center [64], China National Center for Bioinformation/Beijing Institute of Genomics, Chinese Academy of Sciences (GSA-Human: HRA014110) that are publicly accessible at https://ngdc.cncb.ac.cn/gsa-human.

References

[1] D. Armanini, C. Fiore, M.J. Mattarello, J. Bielenberg, M. Palermo, History of the endocrine effects of licorice, Exp. Clin. Endocrinol. Diabetes 110 (2002) 257–261.
[2] S. Shibata, A drug over the millennia: pharmacognosy, chemistry, and pharmacology of licorice, Yakugaku Zasshi 120 (2000) 849–862.
[3] T. Akao, Distribution of enzymes involved in the metabolism of glycyrrhizin in various organs of rat, Biol. Pharm. Bull. 21 (1998) 1036–1044.
[4] S. Krähenbühl, F. Hasler, B.M. Frey, F.J. Frey, R. Brenneisen, R. Krapf, Kinetics and dynamics of orally administered 18 beta-glycyrrhetinic acid in humans, J. Clin. Endocrinol. Metab. 78 (1994) 581–585.
[5] O. Warburg, K. Posener, E. Negelein, Über den Stoffwechsel der Carcinomzelle, Biochem. Z. 152 (1924) 309–344.
[6] O. Warburg, S. Minami, Versuche an Überlebendem Carcinom-gewebe, Klin. Wochenschr. 2 (1923) 776–777.
[7] O. Warburg, Versuche und überledbeudem carcinomgewebe (methoden), Biochem. Z. 142 (1923) 317–333.
[8] O. Warburg, F. Wind, E. Negelein, The metabolism of tumors in the body, J. Gen. Physiol. 8 (1927) 519–530.
[9] E. Negelein, Über die glykolytische Wirkung des embryonalen Gewebes, Biochem. Z. (1925) 162.
[10] C.F. Cori, G.T. Cori, The carbohydrate metabolism of tumors. II. Changes in the sugar, lactic acid, and co-combining power of blood passing through a tumor, J. Biol. Chem. 65 (1925) 397–405.
[11] C.F. Cori, G.T. Cori, The carbohydrate metabolism of tumors. I. the free sugar, lactic acid, and glycogen content of malignant tumors, J. Biol. Chem. 64 (1925) 11–22.
[12] E. Negelein, Versuche über Glykolyse, Biochem. Z. 158 (1925) 121–135.
[13] D.J. Newman, G.M. Cragg, Natural products as sources of new drugs from 1981 to 2014, J. Nat. Prod. 79 (2016) 629–661.
[14] R. Jain, M.A. Hussein, S. Pierce, C. Martens, P. Shahagadkar, G. Munirathinam, Oncopreventive and oncotherapeutic potential of licorice triterpenoid compound glycyrrhizin and its derivatives: molecular insights, Pharmacol. Res. 178 (2022) 106138.
[15] A. Kowalska, U. Kalinowska-Lis, 18beta-Glycyrrhetinic acid: its core biological properties and dermatological applications, Int. J. Cosmet. Sci. 41 (2019) 325–331.
[16] C.S. Lee, Y.J. Kim, M.S. Lee, E.S. Han, S.J. Lee, 18beta-Glycyrrhetinic acid induces apoptotic cell death in SiHa cells and exhibits a synergistic effect against antibiotic anti-cancer drug toxicity, Life Sci. 83 (2008) 481–489.
[17] S. Wang, Y. Shen, R. Qiu, Z. Chen, Z. Chen, W. Chen, 18 beta-glycyrrhetinic acid exhibits potent antitumor effects against colorectal cancer via inhibition of cell proliferation and migration, Int. J. Oncol. 51 (2017) 615–624.

[18] S. Li, J.-H. Zhu, L.-P. Cao, Q. Sun, H.-D. Liu, W.-D. Li, J.-S. Li, C.-H. Hang, Growth inhibitory in vitro effects of glycyrrhizic acid in U251 glioblastoma cell line, Neurol. Sci. 35 (2014) 1115–1120.
[19] H. Yamaguchi, T. Noshita, T. Yu, Y. Kidachi, K. Kamiie, H. Umetsu, K. Ryoyama, Novel effects of glycyrrhetinic acid on the central nervous system tumorigenic progenitor cells: induction of actin disruption and tumor cell-selective toxicity, Eur. J. Med. Chem. 45 (2010) 2943–2948.
[20] Y. Zhang, S. Yang, M. Zhang, Z. Wang, X. He, Y. Hou, G. Bai, Glycyrrhetinic Acid improves insulin-response pathway by regulating the balance between the Ras/MAPK and PI3K/Akt Pathways, Nutrients 11 (2019).
[21] M. Chang, M. Wu, H. Li, Curcumin combined with glycyrrhetinic acid inhibits the development of hepatocellular carcinoma cells by down-regulating the PTEN/PI3K/AKT signalling pathway, Am. J. Transl. Res. 9 (2017) 5567–5575.
[22] Y. Cai, Y. Xu, H.F. Chan, X. Fang, C. He, M. Chen, Glycyrrhetinic acid mediated drug delivery carriers for hepatocellular carcinoma therapy, Mol. Pharm. 13 (2016) 699–709.
[23] F. Wu, X. Li, B. Jiang, J. Yan, Z. Zhang, J. Qin, W. Yu, Z. Gao, Glycyrrhetinic acid functionalized nanoparticles for drug delivery to liver cancer, J. Biomed. Nanotechnol. 14 (2018) 1837–1852.
[24] Y.-q. Sun, C.-m. Dai, Y. Zheng, S.-d. Shi, H.-y. Hu, D.-w. Chen, Binding effect of fluorescence labeled glycyrrhetinic acid with GA receptors in hepatocellular carcinoma cells, Life Sci. 188 (2017) 186–191.
[25] M. Jinek, K. Chylinski, I. Fonfara, M. Hauer, J.A. Doudna, E. Charpentier, A programmable dual-RNA-guided DNA endonuclease in adaptive bacterial immunity, Science 337 (2012) 816–821.
[26] H. Koike-Yusa, Y. Li, E.P. Tan, M.D.C. Velasco-Herrera, K. Yusa, Genome-wide recessive genetic screening in mammalian cells with a lentiviral CRISPR-guide RNA library, Nat. Biotechnol. 32 (2014) 267–273.
[27] O. Shalem, N.E. Sanjana, E. Hartenian, X. Shi, D.A. Scott, T. Mikkelson, D. Heckl, B. L. Ebert, D.E. Root, J.G. Doench, F. Zhang, Genome-scale CRISPR-Cas9 knockout screening in human cells, Science 343 (2014) 84–87.
[28] T. Wang, J.J. Wei, D.M. Sabatini, E.S. Lander, Genetic screens in human cells using the CRISPR-Cas9 system, Science 343 (2014) 80–84.
[29] Y. Zhou, S. Zhu, C. Cai, P. Yuan, C. Li, Y. Huang, W. Wei, High-throughput screening of a CRISPR/Cas9 library for functional genomics in human cells, Nature 509 (2014) 487–491.
[30] J. Shi, Y. Zhao, K. Wang, X. Shi, Y. Wang, H. Huang, Y. Zhuang, T. Cai, F. Wang, F. Shao, Cleavage of GSDMD by inflammatory caspases determines pyroptotic cell death, Nature 526 (2015) 660–665.
[31] O. Shalem, N.E. Sanjana, F. Zhang, High-throughput functional genomics using CRISPR-Cas9, Nat. Rev. Genet. 16 (2015) 299–311.
[32] M.A. Horlbeck, L.A. Gilbert, J.E. Villalta, B. Adamson, R.A. Pak, Y. Chen, A. P. Fields, C.Y. Park, J.E. Corn, M. Kampmann, J.S. Weissman, Compact and highly active next-generation libraries for CRISPR-mediated gene repression and activation, eLife 5 (2016) e19760.
[33] A.P. Halestrap, The monocarboxylate transporter family–Structure and functional characterization, IUBMB Life 64 (2012) 1–9.
[34] A.P. Halestrap, M.C. Wilson, The monocarboxylate transporter family—Role and regulation, IUBMB Life 64 (2012) 109–119.
[35] M.A. Felmlee, R.S. Jones, V. Rodriguez-Cruz, K.E. Follman, M.E. Morris, Monocarboxylate transporters (SLC16): function, regulation, and role in health and disease, Pharmacol. Rev. 72 (2020) 466–485.
[36] V.L. Payen, E. Mina, V.F. Van Hee, P.E. Porporato, P. Sonveaux, Monocarboxylate transporters in cancer, Mol. Metabol. 33 (2020) 48–66.
[37] B. Deuticke, Monocarboxylate transport in erythrocytes, J. Membr. Biol. 70 (1982) 89–103.
[38] C.K. Garcia, X. Li, J. Luna, U. Francke, cDNA cloning of the human monocarboxylate transporter 1 and chromosomal localization of the SLC16A1 locus to 1p13.2-p12, Genomics 23 (1994) 500–503.
[39] L. Carpenter, R.C. Poole, A.P. Halestrap, Cloning and sequencing of the monocarboxylate transporter from mouse Ehrlich Lettré tumour cell confirms its identity as MCT1 and demonstrates that glycosylation is not required for MCT1 function, Biochim. Biophys. Acta 1279 (1996) 157–163.
[40] S. Bröer, A. Bröer, H.P. Schneider, C. Stegen, A.P. Halestrap, J.W. Deitmer, Characterization of the high-affinity monocarboxylate transporter MCT2 in Xenopus laevis oocytes, Biochem. J. 341 (Pt 3) (1999) 529–535.
[41] S. Bröer, H.P. Schneider, A. Bröer, B. Rahman, B. Hamprecht, J.W. Deitmer, Characterization of the monocarboxylate transporter 1 expressed in Xenopus laevis oocytes by changes in cytosolic pH, Biochem. J. 333 (Pt 1) (1998) 167–174.
[42] T. Miyauchi, Y. Masuzawa, T. Muramatsu, The basigin group of the immunoglobulin superfamily: complete conservation of a segment in and around transmembrane domains of human and mouse basigin and chicken HT7 antigen, J. Biochem. 110 (1991) 770–774.
[43] C. Biswas, Y. Zhang, R. DeCastro, H. Guo, T. Nakamura, H. Kataoka, K. Nabeshima, The human tumor cell-derived collagenase stimulatory factor (renamed EMMPRIN) is a member of the immunoglobulin superfamily, Cancer Res. 55 (1995) 434–439.
[44] D. Meredith, A.P. Halestrap, OX47 (basigin) may act as a chaperone for expression of the monocarboxylate transporter MCT1 at the plasma membrane of Xenopus laevis oocytes, J. Physiol. 526 (2000) 23P–24P.
[45] T. Muramatsu, T. Miyauchi, Basigin (CD147): a multifunctional transmembrane protein involved in reproduction, neural function, inflammation and tumor invasion, Histol. Histopathol. 18 (2003) 981–987.
[46] R.C. Poole, A.P. Halestrap, Transport of lactate and other monocarboxylates across mammalian plasma membranes, Am. J. Physiol. 264 (1993) C761–C782.
[47] P. Kirk, M.C. Wilson, C. Heddle, M.H. Brown, A.N. Barclay, A.P. Halestrap, CD147 is tightly associated with lactate transporters MCT1 and MCT4 and facilitates their cell surface expression, EMBO J. 19 (2000) 3896–3904.
[48] H. Chen, L. Wang, J. Beretov, J. Hao, W. Xiao, Y. Li, Co-expression of CD147/EMMPRIN with monocarboxylate transporters and multiple drug resistance proteins is associated with epithelial ovarian cancer progression, Clin. Exp. Metastasis 27 (2010) 557–569.
[49] C. Pinheiro, A. Albergaria, J. Paredes, B. Sousa, R. Dufloth, D. Vieira, F. Schmitt, F. Baltazar, Monocarboxylate transporter 1 is up-regulated in basal-like breast carcinoma, Histopathology 56 (2010) 860–867.
[50] C. Pinheiro, A. Longatto-Filho, K. Simões, C.E. Jacob, C.J.C. Bresciani, B. Zilberstein, I. Cecconello, V.A.F. Alves, F.C. Schmitt, F. Baltazar, The prognostic value of CD147/EMMPRIN is associated with monocarboxylate transporter 1 co-expression in gastric cancer, Eur. J. Cancer 45 13 (2009) 2418–2424.
[51] C. Pinheiro, A. Longatto-Filho, C. Scapulatempo, L. Ferreira, S. Martins, L. Pellerin, M. Rodrigues, V.A. Alves, F. Schmitt, F. Baltazar, Increased expression of monocarboxylate transporters 1, 2, and 4 in colorectal carcinomas, Virchows Arch. 452 (2008) 139–146.
[52] X. Chen, X. Chen, F. Liu, Q. Yuan, K. Zhang, W. Zhou, S. Guan, Y. Wang, S. Mi, Y. Cheng, Monocarboxylate transporter 1 is an independent prognostic factor in esophageal squamous cell carcinoma, Oncol, Rep. 41 (2019) 2529–2539.
[53] G. Zhang, Y. Zhang, D. Dong, F. Wang, X. Ma, F. Guan, L. Sun, MCT1 regulates aggressive and metabolic phenotypes in bladder cancer, J. Cancer 9 (2018) 2492–2501.
[54] M. Leu, J. Kitz, Y. Pilavakis, S. Hakroush, H.A. Wolff, M. Canis, S. Rieken, M. A. Schirmer, Monocarboxylate transporter-1 (MCT1) protein expression in head and neck cancer affects clinical outcome, Sci. Rep. 11 (2021) 4578.
[55] L. Zhang, Z.S. Song, Z.S. Wang, Y.L. Guo, C.G. Xu, H. Shen, High expression of SLC16A1 as a biomarker to predict poor prognosis of urological cancers, Front. Oncol. 11 (2021) 706883.
[56] L. Chen, Y. Li, X. Deng, Comprehensive analysis of pan-cancer reveals the potential of SLC16A1 as a prognostic and immunological biomarker, Medicine 102 (2023) e33242.
[57] X. Guan, M.A. Bryniarski, M.E. Morris, In vitro and in vivo efficacy of the monocarboxylate transporter 1 inhibitor AR-C155858 in the murine 4T1 breast cancer tumor model, AAPS J. 21 (2018) 3.
[58] R.A. Noble, N. Bell, H. Blair, A. Sikka, H. Thomas, N. Phillips, S. Nakjang, S. Miwa, R. Crossland, V. Rand, D. Televantou, A. Long, H.C. Keun, C.M. Bacon, S. Bomken, S.E. Critchlow, S.R. Wedge, Inhibition of monocarboxyate transporter 1 by AZD3965 as a novel therapeutic approach for diffuse large B-cell lymphoma and Burkitt lymphoma, Haematologica 102 (2017) 1247–1257.
[59] R. Polański, C.L. Hodgkinson, A. Fusi, D. Nonaka, L. Priest, P. Kelly, F. Trapani, P. W. Bishop, A. White, S.E. Critchlow, P.D. Smith, F. Blackhall, C. Dive, C.J. Morrow, Activity of the monocarboxylate transporter 1 inhibitor AZD3965 in small cell lung cancer, Clin. Cancer Res. 20 (2014) 926–937.
[60] P. Sonveaux, F. Végran, T. Schroeder, M.C. Wergin, J. Verrax, Z.N. Rabbani, C.J. De Saedeleer, K.M. Kennedy, C. Diepart, B.F. Jordan, M.J. Kelley, B. Gallez, M.L. Wahl, O. Feron, M.W. Dewhirst, Targeting lactate-fueled respiration selectively kills hypoxic tumor cells in mice, J. Clin. Investig. 118 (2008) 3930–3942.
[61] S. Zhu, Z. Cao, Z. Liu, Y. He, Y. Wang, P. Yuan, W. Li, F. Tian, Y. Bao, W. Wei, Guide RNAs with embedded barcodes boost CRISPR-pooled screens, Genome Biol. 20 (2019) 20.
[62] M. Ghandi, F.W. Huang, J. Jané-Valbuena, G.V. Kryukov, C.C. Lo, E.R. McDonald, J. Barretina, E.T. Gelfand, C.M. Bielski, H. Li, K. Hu, A.Y. Andreev-Drakhlin, J. Kim, J.M. Hess, B.J. Haas, F. Aguet, B.A. Weir, M.V. Rothberg, B.R. Paolella, M. S. Lawrence, R. Akbani, Y. Lu, H.L. Tiv, P.C. Gokhale, A. de Weck, A.A. Mansour, C. Oh, J. Shih, K. Hadi, Y. Rosen, J. Bistline, K. Venkatesan, A. Reddy, D. Sonkin, M. Liu, J. Lehar, J.M. Korn, D.A. Porter, M.D. Jones, J. Golji, G. Caponigro, J. E. Taylor, C.M. Dunning, A.L. Creech, A.C. Warren, J.M. McFarland, M. Zamanighomi, A. Kauffmann, N. Stransky, M. Imielinski, Y.E. Maruvka, A. D. Cherniack, A. Tsherniak, F. Vazquez, J.D. Jaffe, A.A. Lane, D.M. Weinstock, C. M. Johannessen, M.P. Morrissey, F. Stegmeier, R. Schlegel, W.C. Hahn, G. Getz, G. B. Mills, J.S. Boehm, T.R. Golub, L.A. Garraway, W.R. Sellers, Next-generation characterization of the cancer cell line encyclopedia, Nature 569 (2019) 503–508.
[63] S. Zhang, X. Chen, E. Jin, A. Wang, T. Chen, X. Zhang, J. Zhu, L. Dong, Y. Sun, C. Yu, Y. Zhou, Z. Fan, H. Chen, S. Zhai, Y. Sun, Q. Chen, J. Xiao, S. Song, Z. Zhang, Y. Bao, Y. Wang, W. Zhao, The GSA family in 2025: a broadened sharing platform for multi-omics and multimodal data, Genom. Proteom. Bioinform. 23 (2025) qzaf072.
[64] C.-N. Members, Partners, database resources of the National Genomics Data Center, China National Center for bioinformation in 2025, Nucleic Acids Res. 53 (2024) D30–D44.
[65] N.J. Curtis, L. Mooney, L. Hopcroft, F. Michopoulos, N. Whalley, H. Zhong, C. Murray, A. Logie, M. Revill, K.F. Byth, A.D. Benjamin, M.A. Firth, S. Green, P. D. Smith, S.E. Critchlow, Pre-clinical pharmacology of AZD3965, a selective inhibitor of MCT1: DLBCL, NHL and Burkitt's lymphoma anti-tumor activity, Oncotarget 8 (2017) 69219–69236.
[66] B.M. Bola, A.L. Chadwick, F. Michopoulos, K.G. Blount, B.A. Telfer, K.J. Williams, P.D. Smith, S.E. Critchlow, I.J. Stratford, Inhibition of monocarboxylate transporter-1 (MCT1) by AZD3965 enhances radiosensitivity by reducing lactate transport, Mol. Cancer Therapeut. 13 (2014) 2805–2816.
[67] S.E. Critchlow, L. Hopcroft, L. Mooney, N. Curtis, N. Whalley, H. Zhong, A. Logie, M. Revill, L. Xie, J. Zhang, D.-H. Yu, C. Murray, P.D. Smith, Abstract 3224: Pre-clinical targeting of the metabolic phenotype of lymphoma by AZD3965, a selective inhibitor of monocarboxylate transporter 1 (MCT1), Cancer Res. 72 (2012), 3224-3224.

[68] R. Plummer, S. Halford, P. Jones, S. Wedge, S. Hirschberg, G. Veal, G. Payne, M. Chenard-Poirier, H. Keun, U. Banerji, A first-in-human first-in-class (FIC) trial of the monocarboxylate transporter 1 (MCT1) inhibitor AZD3965 in patients with advanced solid tumours, Ann. Oncol. 29 (2018) iii9.
[69] R. McNeillis, A. Greystoke, J. Walton, C. Bacon, H. Keun, A. Siskos, G. Petrides, N. Leech, F. Jenkinson, A. Bowron, S. Halford, R. Plummer, A case of malignant hyperlactaemic acidosis appearing upon treatment with the mono-carboxylase transporter 1 inhibitor AZD3965, Br. J. Cancer 122 (2020) 1141–1145.
[70] S.E.R. Halford, H. Walter, P. McKay, W. Townsend, K. Linton, K. Heinzmann, I. Dragoni, L. Brotherton, G. Veal, A. Siskos, H.C. Keun, C. Bacon, S. Wedge, M.J. S. Dyer, E.R. Plummer, Phase I expansion study of the first-in-class monocarboxylate transporter 1 (MCT1) inhibitor AZD3965 in patients with diffuse large B-cell lymphoma (DLBCL) and Burkitt lymphoma (BL), J. Clin. Oncol. 39 (2021), 3115-3115.
[71] N. Wang, X. Jiang, S. Zhang, A. Zhu, Y. Yuan, H. Xu, J. Lei, C. Yan, Structural basis of human monocarboxylate transporter 1 inhibition by anti-cancer drug candidates, Cell 184 (2021) 370–383 e313.
[72] X. Guan, V. Rodriguez-Cruz, M.E. Morris, Cellular uptake of MCT1 inhibitors AR-C155858 and AZD3965 and their effects on MCT-mediated transport of L-lactate in murine 4T1 breast tumor cancer cells, AAPS J. 21 (2019).
[73] A.P. Halestrap, Monocarboxylic acid transport, Compr. Physiol. 3 (2013) 1611–1643.
[74] K. Birsoy, T. Wang, R. Possemato, O.H. Yilmaz, C.E. Koch, W.W. Chen, A. W. Hutchins, Y. Gultekin, T.R. Peterson, J.E. Carette, T.R. Brummelkamp, C. B. Clish, D.M. Sabatini, MCT1-mediated transport of a toxic molecule is an effective strategy for targeting glycolytic tumors, Nat. Genet. 45 (2013) 104–108.
[75] J. Perez-Escuredo, V.F. Van Hee, M. Sboarina, J. Falces, V.L. Payen, L. Pellerin, P. Sonveaux, Monocarboxylate transporters in the brain and in cancer, Biochim. Biophys. Acta 1863 (2016) 2481–2497.
[76] M.C. Wilson, D. Meredith, J.E.M. Fox, C. Manoharan, A.J. Davies, A.P. Halestrap, Basigin (CD147) is the target for organomercurial inhibition of monocarboxylate transporter isoforms 1 and 4, J. Biol. Chem. 280 (2005) 27213–27221.
[77] B. Zhang, Q. Jin, L. Xu, N. Li, Y. Meng, S. Chang, X. Zheng, J. Wang, Y. Chen, D. Neculai, N. Gao, X. Zhang, F. Yang, J. Guo, S. Ye, Cooperative transport mechanism of human monocarboxylate transporter 2, Nat. Commun. 11 (2020) 2429.
[78] Y. Zhang, S. Vaccarella, E. Morgan, M. Li, J. Etxeberria, E. Chokunonga, S. S. Manraj, B. Kamate, A. Omonisi, F. Bray, Global variations in lung cancer incidence by histological subtype in 2020: a population-based study, Lancet Oncol. 24 (2023) 1206–1218.
[79] F. Bray, M. Laversanne, H. Sung, J. Ferlay, R.L. Siegel, I. Soerjomataram, A. Jemal, Global cancer statistics 2022: GLOBOCAN estimates of incidence and mortality worldwide for 36 cancers in 185 countries, Ca - Cancer J. Clin. 74 (2024) 229–263.
[80] J.D. Young, S.Y. Yao, J.M. Baldwin, C.E. Cass, S.A. Baldwin, The human concentrative and equilibrative nucleoside transporter families, SLC28 and SLC29, Mol. Aspect. Med. 34 (2013) 529–547.
[81] R. Zhao, N. Diop-Bove, M. Visentin, I.D. Goldman, Mechanisms of membrane transport of folates into cells and across epithelia, Annu. Rev. Nutr. 31 (2011) 177–201.
[82] R. Zhao, A. Qiu, E. Tsai, M. Jansen, M.H. Akabas, I.D. Goldman, The proton-coupled folate transporter: impact on pemetrexed transport and on antifolates activities compared with the reduced folate carrier, Mol. Pharmacol. 74 (2008) 854–862.
[83] L. Chen, Y. Shu, X. Liang, E.C. Chen, S.W. Yee, A.A. Zur, S. Li, L. Xu, K.R. Keshari, M.J. Lin, H.-C. Chien, Y. Zhang, K.M. Morrissey, J. Liu, J. Ostrem, N.S. Younger, J. Kurhanewicz, K.M. Shokat, K. Ashrafi, K.M. Giacomini, OCT1 is a high-capacity thiamine transporter that regulates hepatic steatosis and is a target of metformin, Proc. Natl. Acad. Sci. U.S.A 111 (2014) 9983–9988.
[84] Y. Shu, S.A. Sheardown, C. Brown, R.P. Owen, S. Zhang, R.A. Castro, A. G. Ianculescu, L. Yue, J.C. Lo, E.G. Burchard, C.M. Brett, K.M. Giacomini, Effect of genetic variation in the organic cation transporter 1 (OCT1) on metformin action, J. Clin. Investig. 117 (2007) 1422–1431.
[85] U.S. Department of Health and Human Services Food and Drug Administration, (CDER), Clinical Drug Interaction studies—study Design, Data Analysis, and Clinical Implications, 2017.
[86] E. Girardi, A. Cesar-Razquin, S. Lindinger, K. Papakostas, J. Konecka, J. Hemmerich, S. Kickinger, F. Kartnig, B. Gurtl, K. Klavins, V. Sedlyarov, A. Ingles-Prieto, G. Fiume, A. Koren, C.H. Lardeau, R. Kumaran Kandasamy, S. Kubicek, G. F. Ecker, G. Superti-Furga, A widespread role for SLC transmembrane transporters in resistance to cytotoxic drugs, Nat. Chem. Biol. 16 (2020) 469–478.